

# ◆ 8 Tb/s Long Haul Transmission Over Low Dispersion Fibers Using 100 Gb/s PDM-QPSK Channels Paired With Coherent Detection

J r mie Renaudier, Oriol Bertran-Pardo, Gabriel Charlet, Massimiliano Salsi, Haik Mardoyan, Patrice Tran, and S bastien Bigo

*100 Gb/s end-to-end broadband optical solutions are attractive to cope with the increasing demand for capacity. Polarization-division-multiplexed (PDM) quaternary-phase-shift-keying (QPSK) paired with coherent detection has been found to be promising for upgrading optical legacy systems based on 50 GHz wavelength slots thanks to its high spectral efficiency (2 bit/s/Hz) and its tolerance to linear effects. One of the major concerns for the deployment of such a solution is the transmission reach, mainly limited by nonlinear effects. This limitation can be exacerbated over non-zero dispersion shifted fiber (NZDSF) due to low local chromatic dispersion of the transmission fiber. The aim of this paper is first to report on the benefits brought by combining coherent detection techniques with advanced modulation formats as compared to conventional direct detection schemes for optical fiber communications. Digital signal processing paired with coherent detection is described to point out the efficiency of a coherent receiver to combat noise and to mitigate linear impairments. We then report on nonlinear tolerance of 100 Gb/s coherent PDM-QPSK through an 8 Tb/s transmission over a dispersion-managed link based on low dispersion fibers.   2010 Alcatel-Lucent.*

## Introduction

While the traffic load of long-haul transport networks currently approaches the maximum link capacities in the vicinity of 1 Tb/s, consisting of roughly 80 to 100 optical channels at 10 Gb/s data rates, commercial network operators foresee a long term trend of traffic growth at rates of 50 percent per year [11], corresponding to a potential 10-fold increase of traffic over six years. To prepare their networks for supporting such traffic growth, carriers have planned to progressively increase the total capacity of their network infrastructure by increasing channel rates from 10 Gb/s

to 40 Gb/s and 100 Gb/s. However, moving from a 10 Gb/s to a 100 Gb/s channel rate is only beneficial in terms of total capacity when the information spectral density is increased simultaneously. The objective of upgrading network capacities by a factor of 10 thus implies that the 10-fold increase in channel rate is compliant with the optical channel spacing of deployed systems, today typically 50 GHz. This requirement gave rise to the emergence of advanced modulation techniques with high spectral efficiency, based on multi-level phase shift encoding and associated

### Panel 1. Abbreviations, Acronyms, and Terms

ADC—Analog-to-digital converter  
BER—Bit error ratio  
CD—Chromatic dispersion  
CPE—Carrier phase estimation  
DCF—Dispersion compensating fiber  
DCM—Dispersion compensating module  
DQPSK—Differential QPSK  
DSF—Dispersion shifted fiber  
FIR—Finite impulse response  
iRZ—Interleaved return-to-zero  
NL—Nonlinear  
NRZ—Non-return-to-zero  
NZ—Non-zero  
OPMDC—Optical polarization mode dispersion compensator

OSNR—Optical signal-to-noise ratio  
PBS—Polarization beam splitter  
PD—Photodiode  
PDM—Polarization division multiplexed  
PMD—Polarization mode dispersion  
PRBS—Pseudo-random bit sequences  
PS—Polarization scrambler  
QPSK—Quadrature phase shift keying  
ROADM—Reconfigurable optical add-drop multiplexer  
RZ—Return-to-zero  
SSMF—Standard single mode fiber  
WDM—Wavelength division multiplexing  
WSS—Wavelength selective switch

with innovative detection techniques, such as differential and coherent detection. Several research publications [1, 6, 9, 16, 19] have thus demonstrated the feasibility of 100 Gb/s wavelength division multiplexed (WDM) long-haul transmissions using polarization division multiplexed quadrature phase shift keying (PDM-QPSK) paired with a coherent receiver. PDM-QPSK is obtained by encoding information over four phase levels, according to the quadrature phase shift keying (QPSK) format, and over two orthogonal polarization states thanks to polarization division multiplexing (PDM). To recover information from the PDM-QPSK modulation format, a coherent receiver including digital signal processing (DSP) presents significant advantages. With respect to direct or differential detection techniques, the advantage of using coherent detection is that coherent receivers take full benefit of powerful DSP to handle polarization division multiplexing, thus enabling a straightforward twofold increase of spectral efficiency, and to mitigate fiber impairments [13, 17, 20, 21, 24]. Indeed, by providing access to all the signal characteristics (polarization, amplitude, and phase), coherent detection enables a dramatic improvement in tolerance to linear fiber impairments at the 100 Gb/s data rate, and more particularly against polarization mode dispersion (PMD), thanks to high-speed processing in the digital domain

[4, 5, 8, 17, 19]. Hence, this solution appears interesting for the upgrade of legacy networks to 100 Gb/s thanks to its spectral efficiency reaching 2bit/s/Hz, consistent with the 50 GHz optical channel spacing of WDM systems.

One of the major concerns for the deployment of such a solution remains the maximum transmission reach, which is mainly limited by the optical signal-to-noise ratio (OSNR) and nonlinear (NL) impairments. Although WDM transmission of 100 Gb/s coherent PDM-QPSK data over distances up to 2,500 km have been reported in pioneering experiments [6, 9, 19] relying on dispersion managed links, these experiments were realized using Raman amplification in order to improve the OSNR at the receiver, and the transmission spans were made of highly dispersive fibers (SSMF or +D/−D). More recently, WDM transmission of 100 Gb/s coherent PDM-QPSK data has been performed under typical terrestrial constraints including EDFA-only amplification and narrow optical filtering resulting from concatenation of reconfigurable optical add-drop multiplexers (ROADMs) across optical networks [1, 19]. Although the weak impact of the concatenation of ROADMs has been demonstrated, the transmission reach appears to decrease to 1,600 km over transmission systems relying on standard single mode fiber (SSMF), having a

chromatic dispersion of 17 ps/nm/km, and dispersion compensating modules (DCMs) to compensate for the accumulated dispersion along the line.

In this paper, we report on the potential of combining a coherent detection technique with advanced modulation formats and digital signal processing to increase information spectral density in optical fiber communication systems. We describe the advantages of the powerful digital signal processing paired with coherent detection to combat noise and to mitigate linear impairments. Finally, we report on the nonlinear tolerance of a 100 Gb/s coherent PDM-QPSK solution through an 8 Tb/s WDM transmission experiment over a dispersion-managed link based on low dispersion fibers. Compared to SSME, the use of low local dispersion fibers, which have a chromatic dispersion of 4 ps/nm/km, may increase nonlinear effects and reduce transmission reach due to their low chromatic dispersion. Therefore, we study the tolerance to intra-channel and inter-channel nonlinear impairments of a 100 Gb/s coherent PDM-QPSK solution. We particularly discuss the benefit of over-modulating PDM-QPSK signals with return-to-zero (RZ) and temporally interleaving by half a symbol period at both polarization tributaries.

### **Advantages of Coherent Receiver Associated With Multilevel Modulation Format and Digital Signal Processing for System Capacity Upgrade of Legacy Optical Networks**

Network operators widely deployed WDM optical networks working at a bit rate of 10 Gb/s between the years 2000 and 2008. Due to the limited bandwidth of current optical amplifiers, these networks usually carry a maximum of 80 to 100 optical channels at 10 Gb/s, representing a maximum capacity in the vicinity of 1 Tbit/sec. Given that the traffic load currently approaches the maximum capacity of these networks, carriers have planned to increase the total capacity of their network infrastructure by increasing channel rates from 10 Gb/s to 100 Gb/s to cope with the expected traffic growth. However, most carriers do not intend to build a specific network for 100 Gb/s applications from scratch, but rather to upgrade them smoothly from 10 Gb/s to 100 Gb/s. In these networks,

light is passed into dispersion compensating fiber (DCF) to avoid a large accumulation of chromatic dispersion within the link, as well as into optical filters within reconfigurable optical add drop multiplexers which are usually designed for systems working with 50 GHz channel spacing at 10 Gb/s. This generates some constraints when moving to 100 Gb/s as these high bit rate channels have to be compatible with the 50 GHz slots defined by the ROADM. As the spectrum is naturally 10 times broader at 100 Gb/s than at 10 Gb/s when the same modulation scheme is applied, the simplest modulation format—non return-to-zero (NRZ)—can no longer be used. The spectrum occupancy of the signal is around twice the symbol rate, i.e., 200 GHz at 100 Gb/s. For this reason, increasing the capacity transmitted within a fiber optic-based system with a 50 GHz spacing grid requires increasing the information spectral density (i.e., the number of bits per second transmitted in a unit spectral band). To address this issue of keeping constant optical bandwidth while increasing bit rate, effective solutions based on advanced modulation formats have been developed to increase the number of bits carried per symbol. First, modulation formats with 2 bits per symbol were proposed [10], either with four phase levels such as QPSK, or with four amplitude levels (even though the latter did not generate significant interest due to its poor tolerance to optical noise). Recently, a modulation format transmitting 4 bits per symbol has attracted a lot of interest. By combining polarization multiplexing and four phase levels, PDM-QPSK [23] is seen as extremely promising for high capacity 100 Gb/s transmission [1, 6, 9, 16, 19].

Polarization division multiplexing, which was used in 2001 and 2002 in “record laboratory experiments” in order to increase system capacity by a factor of 2, has been almost completely abandoned due to the practical difficulties of implementation, the poor cost-efficiency of this solution, and impairments caused either by linear effects such as depolarization induced by PMD [14], by nonlinear effects such as depolarization induced by cross phase modulation [26], or by the necessity of a high performance polarization tracking component at the receiver side. The application of coherent detection (abandoned in the

early 1990s), in combination with polarization division multiplexing (abandoned 10 years later), is currently regaining strong interest due to the availability of powerful digital signal processing electronics and algorithms, especially for 100 Gb/s transmissions. Using this technique, a very high information spectral density of 2 bit/s/Hz is achieved, allowing channels at 100 Gb/s to be packed onto the 50 GHz channel spacing grid of existing networks. Several papers have already demonstrated the feasibility of carrying 100 Gb/s coherent PDM-QPSK channels over existing WDM transmission systems with 50 GHz spacing grid [1, 6, 9, 16, 19]. **Figure 1** illustrates a nine channel spectrum carrying 100 Gb/s data spaced by 50 GHz in which we can observe that the channel overlap is very low as dips between two adjacent channels are as high as 30 dB. This demonstrates the efficiency of the PDM-QPSK modulation format to increase the total capacity of deployed WDM systems, especially when it is combined with a coherent receiver.

### Polarization Diversity Coherent Receiver

A coherent receiver, schematized in **Figure 2**, aims at generating in-phase and in-quadrature components from a received signal along the two orthogonal states of polarization of the incoming light. The coherent receiver combines the light from the received signal with that of a local oscillator, which acts as a

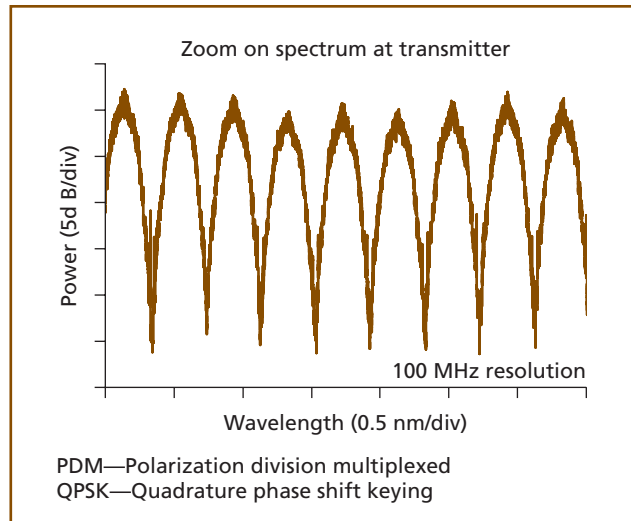


**Figure 1.** Experimental optical spectrum representing 100 Gb/s PDM-QPSK channels packed onto a 50 GHz spacing grid.

pure reference phase signal. The local oscillator usually consists of a continuous wave laser oscillating at a frequency very close to that of the optical carrier of the received signal.

A key component used within a coherent receiver is a “coherent mixer,” which produces interference between a local oscillator and the incoming signal. In order to generate in-phase and in-quadrature

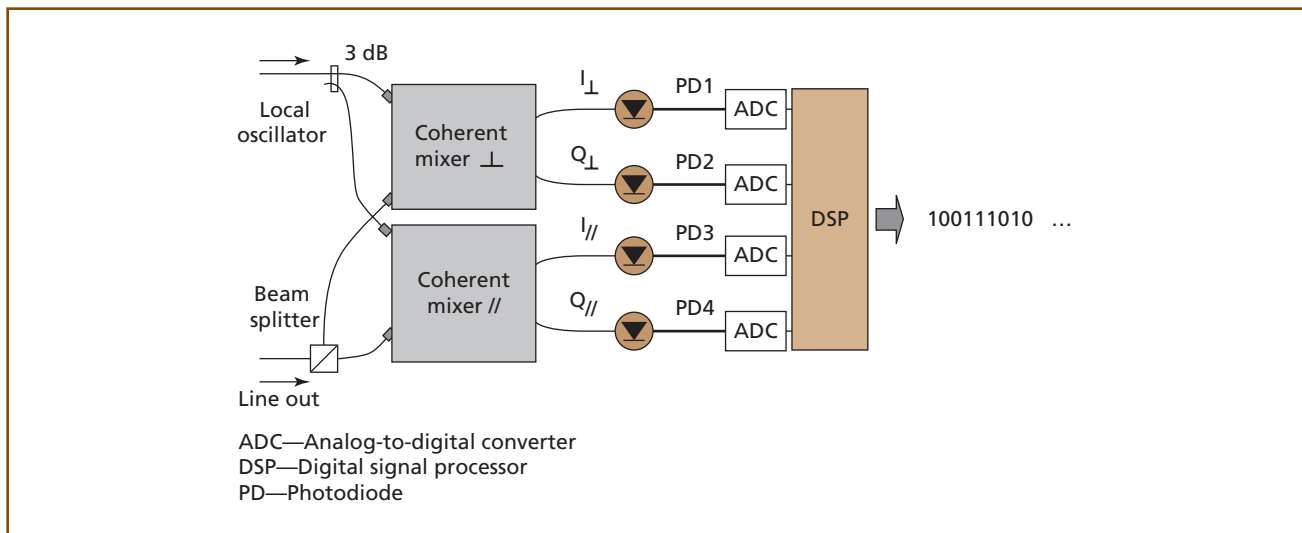


**Figure 2.** Schematic description of a polarization diversity coherent receiver.

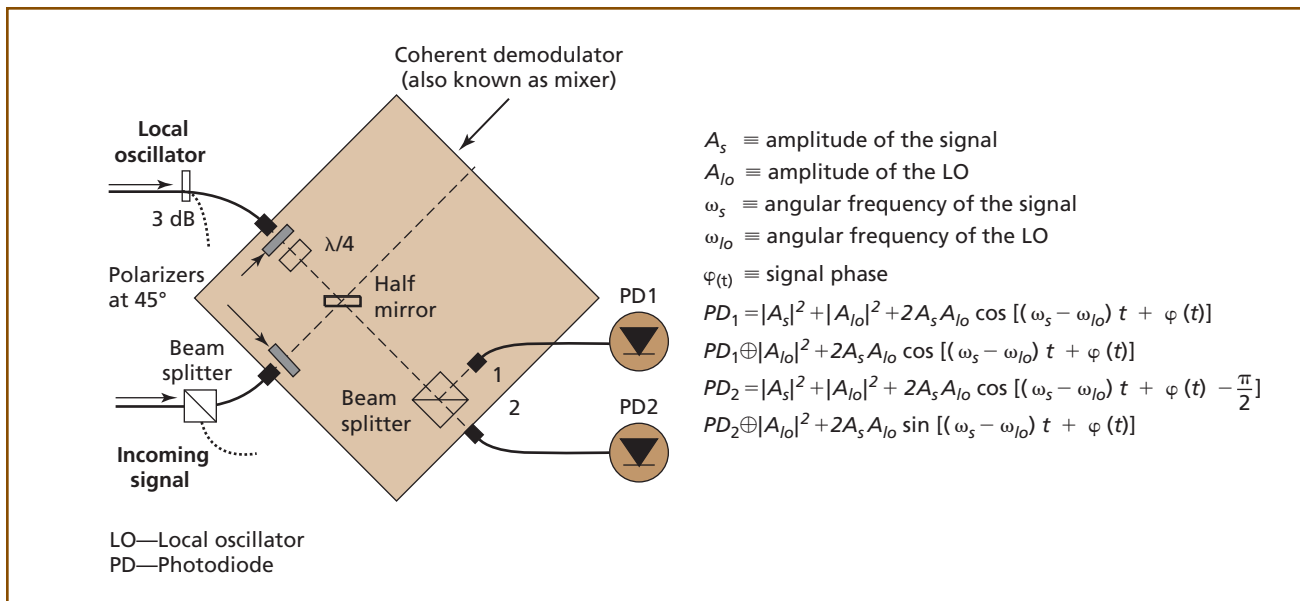


**Figure 3.**  
**Coherent mixer description.**

components of the product “signal  $\times$  local oscillator,” the local oscillator is divided into two parts having a 90 degree relative phase shift. The local oscillator has an optical frequency  $f_{l_0}$  while the carrier frequency of the signal is  $f_s$ , slightly different from  $f_{l_0}$ , typically by few hundreds of MHz. Different architectures are proposed for the realization of an optical coherent mixer. **Figure 3** describes a schematic architecture of a coherent mixer based on free space optics technologies. Collimators are used to send light from the optical fiber to this free space device. The polarizations of the signal and of the local oscillator are both at 45 degrees to the figure plan. A  $\lambda/4$  wave plate is used to generate the 90 degree phase shift between the horizontal and the vertical components of the electrical field. A wave splitter plate, with a 50 percent reflection ratio, is then used to combine the local oscillator and the signal together. Two polarization beam splitters (PBS) are then inserted in order to generate a total of four signals, which are then sent to photodiodes, for optical-to-electrical conversion. Only two photodiodes can be used if the power of the local oscillator is much larger than the one of the signal, as shown in the equations in Figure 3, since the term  $|A_s|^2$  becomes

negligible compared to the product  $A_s A_{l_0}$ . Photodiode 1 (PD1) provides access to the cosine of the phase information  $\varphi(t)$ , while the sine of the phase information is available simultaneously on photodiode 2 (PD2), provided that the difference in pulsation ( $\omega_s - \omega_{l_0}$ ) between the local oscillator and the signal is recovered as described in the Figure 3 equations. The difference in pulsation ( $\omega_s - \omega_{l_0}$ ) between the two optical signals can be cancelled out by digital signal processing if its own variation is slow enough compared to the symbol rate. Signal phase  $\phi(t)$  can then be reconstructed and data encoded at the transmitter side can be recovered.

In order to recover the full electrical field of the incoming optical signal, a polarization diversity scheme is used, as shown in Figure 2. The light from the incoming signal is first split into two parts by a polarization beam splitter (PBS), and each part is sent into a distinct coherent mixer followed by photodetection to generate the in-phase and quadrature components of the signal along the two received states of polarization. The four optical interference waveforms generated by photodetection are then sampled, digitized by analog-to-digital converters (ADCs), and post-processed as described in the next section.



## Digital Signal Processing Sampling

According to the Shannon-Nyquist criterion, the received signal should be sampled at a rate of at least twice its bandwidth. Practically, in a transponder specially designed for coherent systems, the 3 dB bandwidth of the ADC is roughly 0.5 to 0.8 times the symbol rate, and the ADC sampling rate is exactly twice the symbol rate. Nevertheless, sampling heads used in most of the research experiments have a 3 dB bandwidth of 16 GHz and work at a fixed sampling rate slightly lower than twice the symbol rate. Here, this sampling rate is 50 Gsamples/s for a symbol rate of 28 Gbaud as noted in [6] and [9]. Consequently, digitized signals have roughly 1.8 samples per symbol. In order to have DSP operating at exactly two samples per symbol, the first step is to resample the digital signal using an interpolation technique.

## Chromatic Dispersion Compensation

Chromatic dispersion (CD) is a static polarization-independent phenomenon that can be compensated for before equalizing and demultiplexing the received signal to recover the two orthogonal polarization tributaries sent at the transmitter side. Thus, since we roughly know the residual amount of chromatic dispersion, we use the well-known analytical expression of CD to design the filter which compensates for it. This expression is

$$G(z, \omega) = \exp\left(-j \frac{D\lambda^2}{4\pi c} \omega^2\right)$$

where  $z$  is the distance,  $\omega$  is the angular frequency,  $j$  is the imaginary unit,  $D$  is the dispersion coefficient of the fiber,  $\lambda$  is the wavelength, and  $c$  is the speed of light. The practical implementation of the digital filter corresponding to such an expression is impossible because its response is not causal and has an infinite duration. Practically, the response is truncated and static finite impulse response (FIR) filters are used. The length of these filters is proportional to the amount of CD to be compensated for. For practical real-time implementation, the amount of CD compensation will depend on the calculation capacity of the state-of-the-art technologies.

## Equalization and Polarization Demultiplexing

A key part of the DSP is demultiplexing the received signal to recover the two orthogonal polarization

tributaries sent at the transmitter side. This can be done using blind adaptive FIR filters, updated using the stochastic gradient constant modulus algorithm (CMA) as proposed in [23]. The filters are arranged in a butterfly structure (as seen in **Figure 4**) and are continuously updated to follow channel perturbations such as polarization-dependent fluctuations, or PMD. The impact of all these perturbations can be modeled as a Jones matrix. It has to be noted that the two input signals of the block,  $x_{in}$  and  $y_{in}$ , are a mix of the two signals emitted along the two orthogonal states of polarization of the light. Therefore the task of the equalizer is to estimate the inverse of the Jones matrix so as to reverse the effects induced by the channel propagation. The output signal is obtained as follows:

$$x_{out} = h_{xx} \cdot x_{in} + h_{xy} \cdot y_{in}$$

$$y_{out} = h_{yx} \cdot x_{in} + h_{yy} \cdot y_{in}$$

where  $x_{in}$  and  $y_{in}$  are the input signals,  $x_{out}$  and  $y_{out}$  are the output signals, and  $h_{xx}$ ,  $h_{xy}$ ,  $h_{yx}$ , and  $h_{yy}$  are the adaptive FIR filters having T/2-spaced complex tap-coefficients (also known as taps). These coefficients are updated such that

$$h_{xx} \rightarrow h_{xx} + \mu \varepsilon_x x_{out} \cdot x_{in}^*$$

$$h_{xy} \rightarrow h_{xy} + \mu \varepsilon_y y_{out} \cdot y_{in}^*$$

$$h_{yx} \rightarrow h_{yx} + \mu \varepsilon_x x_{out} \cdot x_{in}^*$$

$$h_{yy} \rightarrow h_{yy} + \mu \varepsilon_y y_{out} \cdot y_{in}^*$$

where  $\mu$  is the convergence parameter,  $x_{in}^*$  and  $y_{in}^*$  are the complex conjugate of  $x_{in}$  and  $y_{in}$ , respectively, and the error terms which have to be minimized are given by

$$\varepsilon_x = 1 - |x_{out}|^2$$

$$\varepsilon_y = 1 - |y_{out}|^2$$

for unit amplitude signals. At the end of this DSP block, the two output signals,  $x_{out}$  and  $y_{out}$ , are polarization-demultiplexed and equalized using the estimated Jones matrix.

It must be noted here that using complex tap-coefficients, a 13-tap adaptive equalizer can also mitigate for residual chromatic dispersion of up to  $\pm 750$  ps/nm at 100 Gb/s [9]. This result suggests that

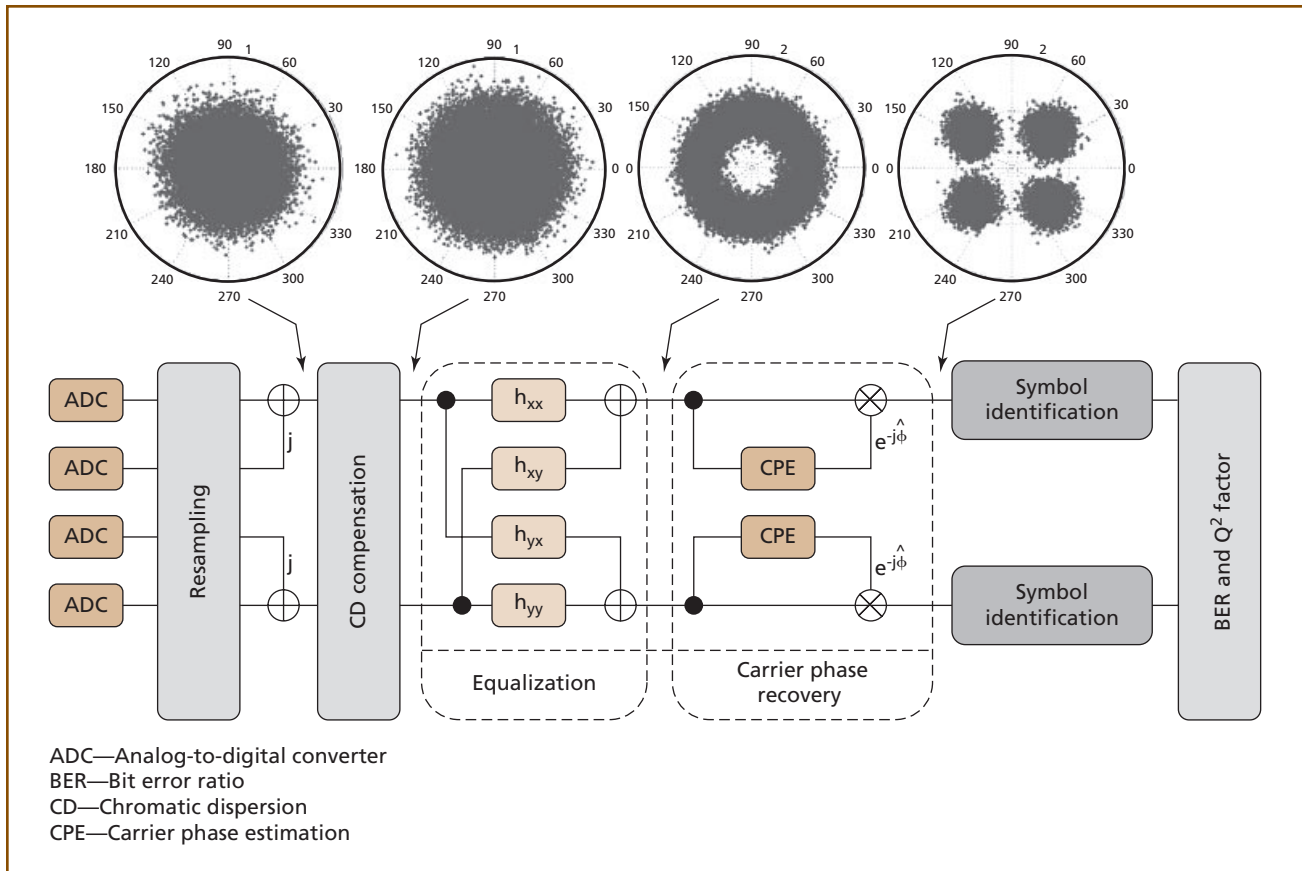


**Figure 4.**  
**Digital signal processing done in coherent receiver.**

such a simple DSP without the large filter required for significant CD compensation inserted before polarization demultiplexing would be sufficient to provide very good mitigation of residual dispersion impairments in most legacy optical networks relying on dispersion management with periodically distributed dispersion compensating modules.

Once the two polarization tributaries have been separated by the blind adaptive equalizer, phase-tracking has to be done in the digital domain since the local oscillator is not optically phase-locked onto the received signal. Otherwise, the constellation diagram expected (four clouds located at  $+\pi/4$ ,  $+3\pi/4$ ,  $-3\pi/4$ , and  $-\pi/4$ ) would look like a thick circle, as it appears at the output of the polarization demultiplexing stage in Figure 4. This phase offset will be recovered by the following block in the DSP.

### Carrier Phase Estimation

This process is used to recover and subsequently remove the remaining phase mismatch,  $\phi$ , between the local oscillator and the signal. As the previous adaptive algorithm acts as a fine clock recovery block as well, the estimation of this mismatch is done on the “central” sample only (while the other one is dropped) by using a nonlinear carrier phase tracking algorithm [27] as follows: first, the  $M$ -th power of the complex symbol is taken in order to remove any information encoded in the phase of the signal ( $M$  being the number of phase levels of the modulation, i.e., four for a QPSK modulation). Second, an averaging window of  $N + 1$  elements is computed by summing the result over  $N/2$  pre-cursor and  $N/2$  post-cursor symbols. Then, the argument is taken since we are only interested in the phase. Finally, as shown by

the equation below, the resulting phase is divided by  $M$  to correct for the initial elevation to the  $M$ -th power and subsequently unwrapped to obtain results in the range  $[-\pi, \pi]$ .

$$\hat{\phi}(k) = \frac{1}{M} \arg \left[ \sum_{p=-N/2}^{N/2} x_{out}^M(k+p) \right]$$

This step has been shown to be critical since a correct estimation of the phase depends on the number of consecutive symbols considered [3, 25]. In fact, when transmission performance is limited mainly by optical noise, high values of  $N$  can be employed to obtain better performance. In contrast, when nonlinear effects become dominant during the transmission, a smaller number of consecutive symbols should be considered to follow fast variations of the phase, thus reducing the accuracy of the phase estimation.

It has to be noted here that, as pointed out in [12], phase estimators perform well when estimated phase can be considered as unbiased in the range of the chosen averaging window, leading to the following condition on the frequency detuning,  $\Delta f$ , between the carrier of the received signal and the frequency of the local oscillator:

$$\Delta f \leq \frac{1}{2(N+1)MT_s}$$

where  $T_s$  is the sampling period,  $N+1$  is the averaging window for carrier phase estimation (CPE), and  $M$  is the number of symbol states. According to this condition, the maximum tolerable frequency offset is around  $\pm 600$  MHz for 100 Gb/s PDM-QPSK operating at 28 Gbaud. Since the accuracy of typical temperature-stabilized lasers is around  $\pm 1$  GHz, a technique derived from the nonlinear carrier phase tracking algorithm and presented in [12] is usually performed to estimate and remove the frequency detuning,  $\Delta f$ , before processing CPE.

### Symbol Identification and Bit Error Ratio Calculation

After carrier phase estimation, the digital signal is ready to be processed by the decision block. The threshold decision on each symbol is realized while differential decoding is used to avoid the possibility of cycle slips. Finally, we compare the extracted pattern with the original sequence, and errors are found and counted. This results in a bit error ratio (BER).

**Table I. Relation between BER and  $Q^2$  factor.**

BER	$Q^2$ factor
$1 \cdot 10^{-9}$	15.6
$1 \cdot 10^{-6}$	13.6
$1 \cdot 10^{-5}$	12.6
$1 \cdot 10^{-4}$	11.4
$1 \cdot 10^{-3}$	9.9
$4 \cdot 10^{-3}$	8.6

BER—Bit error ratio

For practical reasons, the system performance measured is usually not expressed in BER but in  $Q^2$  factor. The direct relationship between the BER and the  $Q^2$  factor in dB is presented in **Table I**.

### Efficiency of Coherent Detection to Combat Noise and to Mitigate Linear Impairments

Coherent receivers enjoy the high sensitivity associated with homodyne detection but with the added benefit of advanced digital signal processing (DSP) that offers the possibility to compensate for linear impairments such as chromatic dispersion (CD) and polarization mode dispersion (PMD). In that respect, the remarkable tolerance of coherent receivers against optical noise [13, 24], chromatic dispersion [22, 23], as well as polarization mode dispersion [17, 20] have been reported in the literature. All these features highlight the potential of coherent detection to develop high bit rate solutions that meet the system requirements defined for conventional 10 Gb/s NRZ-based systems.

### Improved Tolerance to Optical Noise Brought by the Use of a Coherent Receiver

When coherent detection is used, the OSNR sensitivity closely approaches the fundamental limit predicted by digital communications theory, and thus cannot be much further improved. With BPSK modulation, the advantage over differential detection is around 1 dB (as the reference signal comes from a pure local oscillator instead of the noisy previous bit). The same OSNR sensitivity is obtained with BPSK and QPSK modulation schemes when coherent detection is used, contrary to differential detection. The advantage



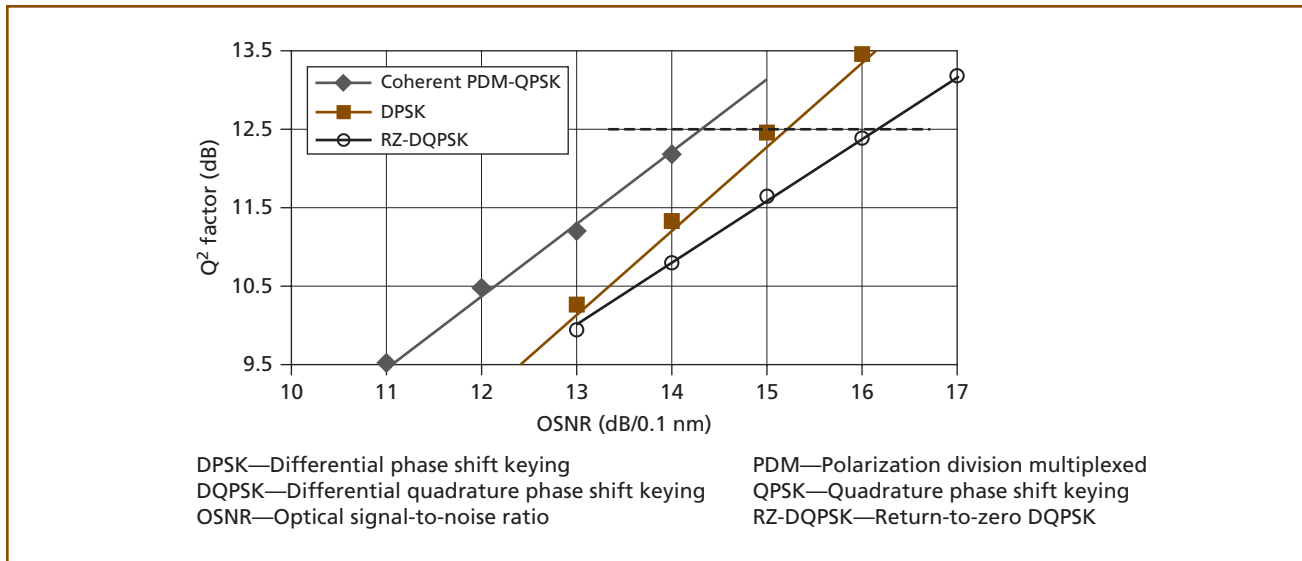


**Figure 5.** Measurement of OSNR sensitivity of coherent PDM-QPSK, DPSK and RZ-DQPSK at 40 Gb/s.

of QPSK combined with coherent detection over the differential detection scheme is therefore around 2.5 dB [15].

Moreover, coherent detection can easily handle a polarization division multiplexed format, without any penalty, by implementing the polarization demultiplexing process in the digital domain. Hence PDM-QPSK has the same sensitivity as QPSK and BPSK (at the same bit rate), all being near the fundamental limit of digital communications. OSNR sensitivity measurements of coherent PDM-QPSK, DPSK, and RZ-DQPSK are presented at 40 Gb/s in **Figure 5**. All measurements are 1 dB or 2 dB away from the theoretical expectations due to implementation penalties. Nevertheless, when comparing OSNR sensitivity at a  $Q^2$  factor of 12.5 dB (corresponding to a BER of  $1 \cdot 10^{-5}$ ), coherent PDM-QPSK is 1 dB better than DPSK, which is also 1 dB better than RZ-DQPSK (RZ over modulation, slightly improving the experimental OSNR sensitivity of DQPSK).

### Compensation of Linear Impairments in a Coherent Receiver

Several impairments are associated with fiber optic propagation. These impairments may be split into two main categories: linear impairments and

nonlinear impairments. Linear impairments correspond to distortions of the electrical field amplitude and phase which can be modeled by a linear filter. Hence, impairments such as chromatic dispersion and polarization mode dispersion can be represented by an all pass filter (i.e., no loss of signal). The inverse filter can thus be calculated, within the coherent receiver, to undo the deformations introduced by propagation. This is the main motivation for the introduction of coherent detection in optical communications.

**Chromatic dispersion compensation.** Chromatic dispersion has been managed for a WDM system working at 10 Gb/s and 40 Gb/s primarily by using optical methods such as dispersion compensating fiber, fiber bragg gratings (FBGs), or etalon-based structures. At 10 Gb/s, most of the installed systems rely on DCF, inserted within the interstage of dual-stage amplifiers along the line. The optical module is thus shared between all the WDM channels. At 40 Gb/s, the same strategy is used, but due to some dispersion uncertainties and dispersion slope mismatch between DCF and line fiber within the WDM band, tunable dispersion compensation systems are usually inserted in each receiver to finely adjust the residual dispersion before intensity detection with a photo-receiver.

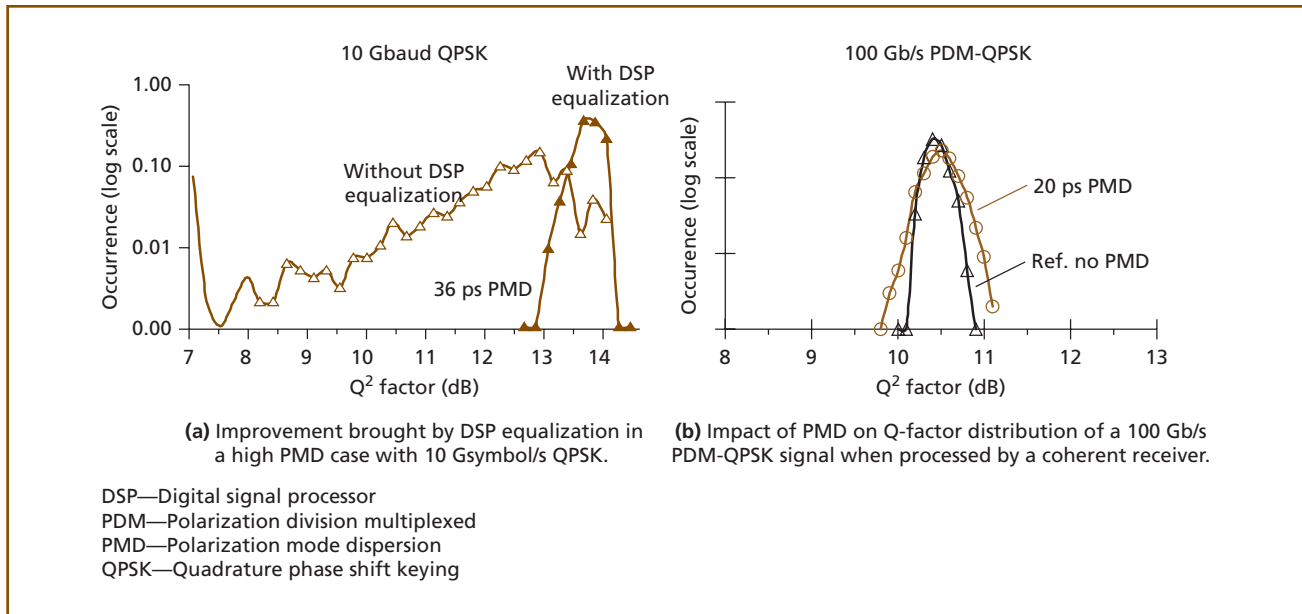


**Figure 6.** Digital signal processing inside a coherent receiver can compensate for PMD.

A coherent receiver detects the amplitude and the phase of the optical field. Thus, coherent detection offers the possibility to compensate for chromatic dispersion through digital signal processing by digitally applying the correct reverse filter. Therefore tunable optical compensators can be removed, and DCFs in the line are also no longer required. Demonstration of 100 Gb/s transmission over links without dispersion-compensating modules has been reported over several thousand kilometers [7] by using coherent detection and digital signal processing.

**Polarization mode dispersion compensation.** Polarization mode dispersion is another major linear limitation of optical communications. Recent fibers have very low PMD, around  $0.05 \text{ ps/km}^{1/2}$ . Nevertheless, fiber deployed before 1995 may suffer from very large PMD values, sometimes higher than  $1 \text{ ps/km}^{1/2}$ . Typical 10 Gb/s systems are limited by PMD when the total PMD in the link reaches 10 ps to 16 ps. At 40 Gb/s, the PMD constraints are four times tighter, and the maximum PMD tolerated is around 2.5 ps to 4 ps. This is a major problem for 40 Gb/s deployment. The first solution proposed for 10 Gb/s systems, namely, the optical polarization mode dispersion compensator (OPMDC), which was not adopted initially due to cost, but is now recommended again. The OPMDC is able to

compensate for the PMD impact but only to a certain extent, and it does not work for all the WDM channels simultaneously, so one OPMDC has to be included within each receiver. Hence this solution is costly, but it allows managing PMD impact up to  $\sim 8$  ps at 40 Gb/s.

At higher bit rates, the PMD problem is even more severe and no satisfactory solution to mitigate high PMD values at low cost had been proposed until the advent of coherent detection. **Figure 6** illustrates how the use of powerful digital signal processing inside a coherent receiver can compensate for a very large amount of PMD. In Figure 6a, the impact of adaptive equalization provided by digital signal processing through a CMA-based algorithm is depicted. A 10 Gsymbol/s QPSK signal was passed through a 400 km long transmission line with a PMD value as high as 36 ps, and the signal was recorded at the receiver side. While the white triangles represent the  $Q^2$  factor distribution with no equalization processing, the dark triangles depict the performance obtained when equalization was switched on. With equalization, the  $Q^2$  factor stayed above 11.5 dB, while it can be reduced below 7 dB in the absence of equalization. In Figure 6b, the impact of PMD on a 100 Gb/s PDM QPSK signal is shown for low PMD values ( $< 1$  ps) and high PMD values (20 ps) [4, 17].

Typically, 10 Gb/s standard systems can tolerate nearly 12 ps PMD. Here, by using coherent detection and digital signal processing, a higher amount of PMD may be tolerated for a 100 Gb/s signal (which could be expected to be 10 times less tolerant than a 10 Gb/s one). We observe that the  $Q^2$  factor distribution is only slightly distorted, and that the performance degradation is low (less than 0.5 dB when the lower tail of the distribution is observed).

### Coherent Systems for 100 Gb/s Long Haul Transmission

The association of coherent detection with powerful digital signal processing is a key method to increase information spectral density up to 2 bit/s/Hz [6, 9], while containing linear distortions induced by optical fiber propagation (chromatic dispersion and PMD). Nevertheless, a good tolerance to nonlinear effects is required to allow transmission over long distances, a key feature for a cost-effective optical network. Indeed, on top of linear fiber effects and optical noise, optical communications may be limited by nonlinear fiber effects originating mainly from the Kerr effect. Nonlinear impairments may cause penalties depending on bit rates, modulation formats, and detection techniques. As an example, on the one hand, it has been demonstrated that the coherent PDM-QPSK solution suffers from large penalties at 40 Gb/s arising from inter-channel effects [3, 25], severely limiting the maximum achievable transmission reach. On the other hand, the increase in the bit rate from 40 Gb/s to 100 Gb/s naturally helps in reducing inter-channel related impairments [2], and several reports have demonstrated the feasibility of 100 Gb/s coherent PDM-QPSK long haul transmission, especially over dispersion-managed systems relying on standard single mode fiber, having a CD of 17 ps/nm/km around 1550 nm, and a periodic DCM to compensate for the accumulated dispersion along the line [1, 16, 19]. Compared to SSF, the use of low dispersion fiber may emphasize nonlinear effects by reducing the walk-off between adjacent channels. In the following experiment, we investigate an 8 Tb/s transmission using 100 Gb/s coherent PDM-QPSK solution over non-zero dispersion shifted fiber (NZ-DSF) based systems, i.e., with a CD of approximately

4 ps/nm/km around 1550 nm, and we study its tolerance to intra-channel and inter-channel nonlinear impairments.

### Experimental Setup

The experiments carried out here involve either single-channel transmission, or homogeneous WDM transmission in which all channels have the same modulation format and bit rate. Two configurations are thus used successively at the transmitter side, as shown in **Figure 7**. In both configurations, the test channel (at 1546.52 nm) is PDM-QSPK modulated at 100 Gb/s. On the contrary, the surrounding channels can be either kept continuous or PDM-QPSK modulated at 100 Gb/s corresponding, respectively, to the single-channel or homogeneous WDM transmissions.

As depicted, our transmitter consists of 82 DFB lasers, spaced by 50 GHz and separated into two spectrally interleaved combs which are independently modulated. To generate the PDM-QPSK data, the light from each comb is sent to a different QPSK modulator operating at 28 Gbaud (i.e., 56 Gb/s). The modulators are fed by  $2^{15}-1$  bit-long pseudo-random bit sequences (PRBS) at 28 Gb/s, including forward error correction (FEC) and protocol overhead. When RZ modulation is desired, the QPSK data are then passed through a 50 percent RZ pulse carver operating at 28 GHz in order to produce 28 Gbaud RZ-QPSK signals. Polarization multiplexing is finally performed by dividing, decorrelating, and recombining the (RZ-) QPSK data through a polarization beam combiner (PBC) with an approximate 300 symbol delay, yielding (RZ-) PDM-QPSK data at 112 Gb/s.

Here, by adjusting a polarization-maintaining delay line with appropriate lengths before the PBC, the two orthogonal polarization tributaries can be either temporally aligned or interleaved by half a symbol ( $\sim 18$  ps). In the rest of the paper, *i*RZ-PDM-QPSK stands for orthogonal RZ-QPSK polarization tributaries interleaved by half a symbol, and NRZ-PDM-QSPK refers to the case when orthogonal NRZ-QPSK polarization tributaries are pulse-to-pulse aligned. The corresponding schematic forms of the signals in the time domain and eye diagrams are shown in **Figure 8**. In the *i*RZ-PDM-QPSK configuration in **Figure 8a**, when polarization tributaries are interleaved by half a symbol,

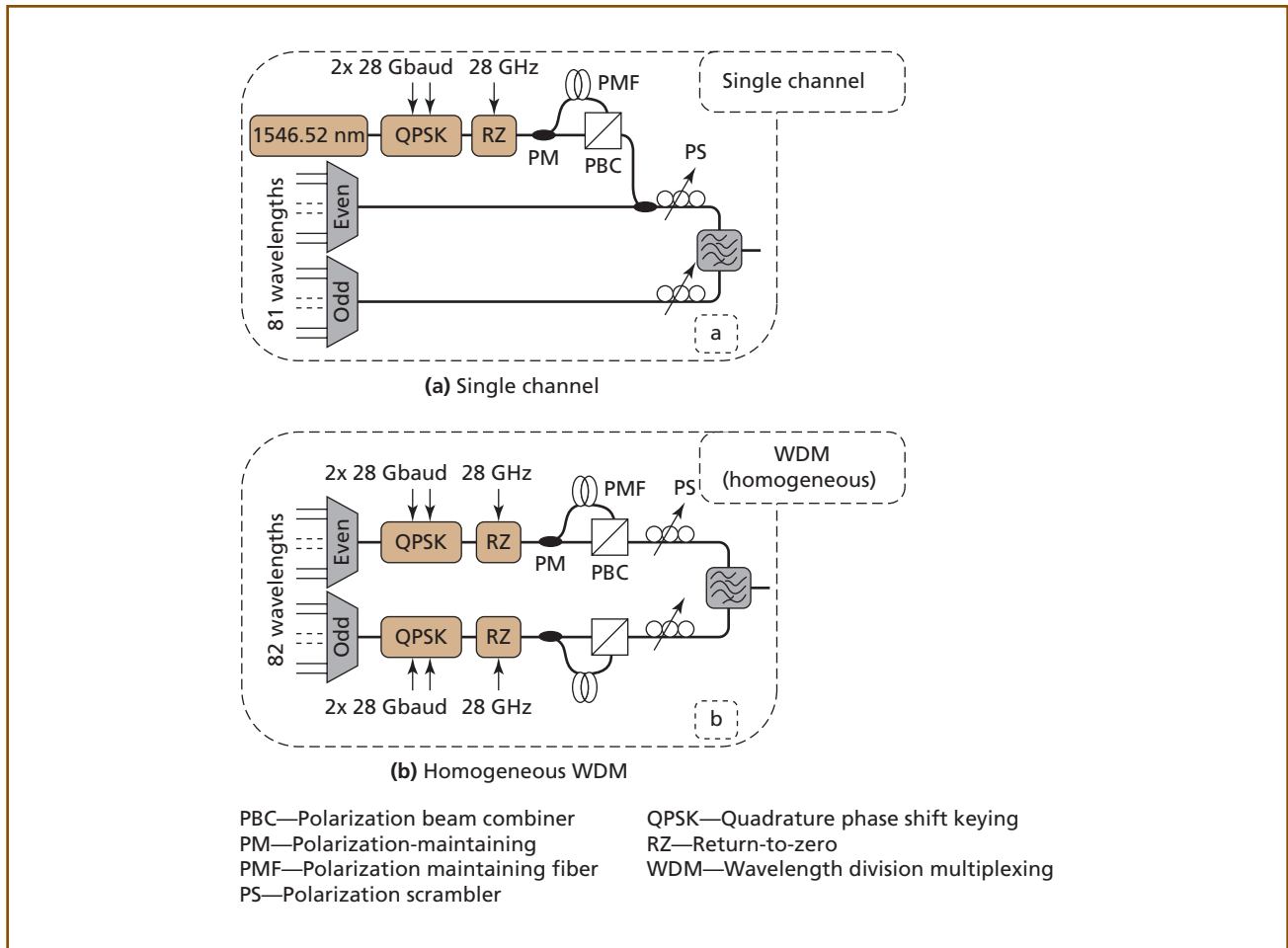


**Figure 7.** Experimental transmitter setup for the two different configurations.

a nearly constant channel power is measured, as shown in the upper-right inset. On the contrary, when the NRZ-QPSK tributaries are temporally aligned, the eye diagram clearly defines intensity transitions between different phase states, a characteristic of LiNbO<sub>3</sub>-based nested QPSK modulators, as shown in Figure 8b.

In any case, the two generated combs are passed into a low-speed (<10 Hz) polarization scrambler (PS) and combined with a 50 GHz interleaver. The resulting multiplex is boosted by a dual-stage EDFA incorporating dispersion compensating fiber for pre-compensation and sent into the recirculating loop. The recirculating loop, depicted in **Figure 9**, incorporates four 100

km-long spans of NZ-DSF which are separated by dual-stage EDFA including an adapted spool of DCF for partial dispersion compensation, according to a typical dispersion map for terrestrial transmission. A wavelength selective switch (WSS) is also inserted at the end of the loop to perform channel power equalization and to emulate optical filtering and crosstalk stemming from nodes in a transparent network. This is done by passing odd and even channels through distinct output ports, introducing an additional optical path to even channels for further decorrelation before recombining them in a 3 dB coupler.

We measure the performance after different transmission distances by changing the number of

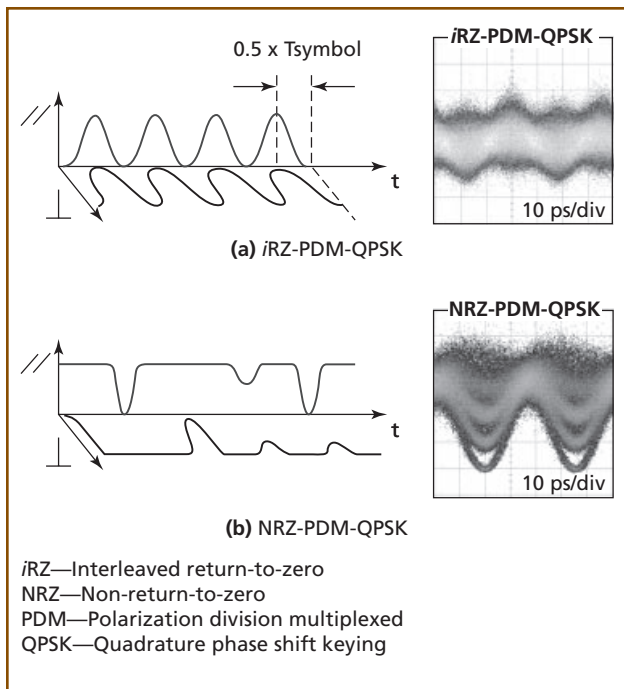


**Figure 8.**  
*Typical shape of the signal in the time domain and experimental eye diagrams.*

loop round-trips and we vary the power per channel,  $P_{ch}$ , at each fiber input by changing the output power of the amplifiers from 13 dBm to 18 dBm while keeping the number of channels constant at 82 channels. Since the maximum output power of the amplifiers is 18 dBm, we reduce the number of channels to extend the studied power range, when necessary. In all experiments, we chose to set the launch power of the test channel at the same level as all the co-propagating channels.

At the receiver side, the channel under study is selected by a 0.4 nm bandwidth filter and sent into the coherent receiver. The signals from the coherent receiver are detected by four balanced photodiodes, digitized by four analog-to-digital converters of an oscilloscope, at 50 Gsamples/s with a 16 GHz electrical bandwidth, and stored as sets of 2,000,000 samples (which correspond to a time slot of 40  $\mu$ s), which is the maximum storage capacity on the 50 GS/s high speed sampling oscilloscope. In this condition, a minimum BER of  $2.5 \times 10^{-5}$  can be computed for each set of samples with a high confidence level. Thus, in our

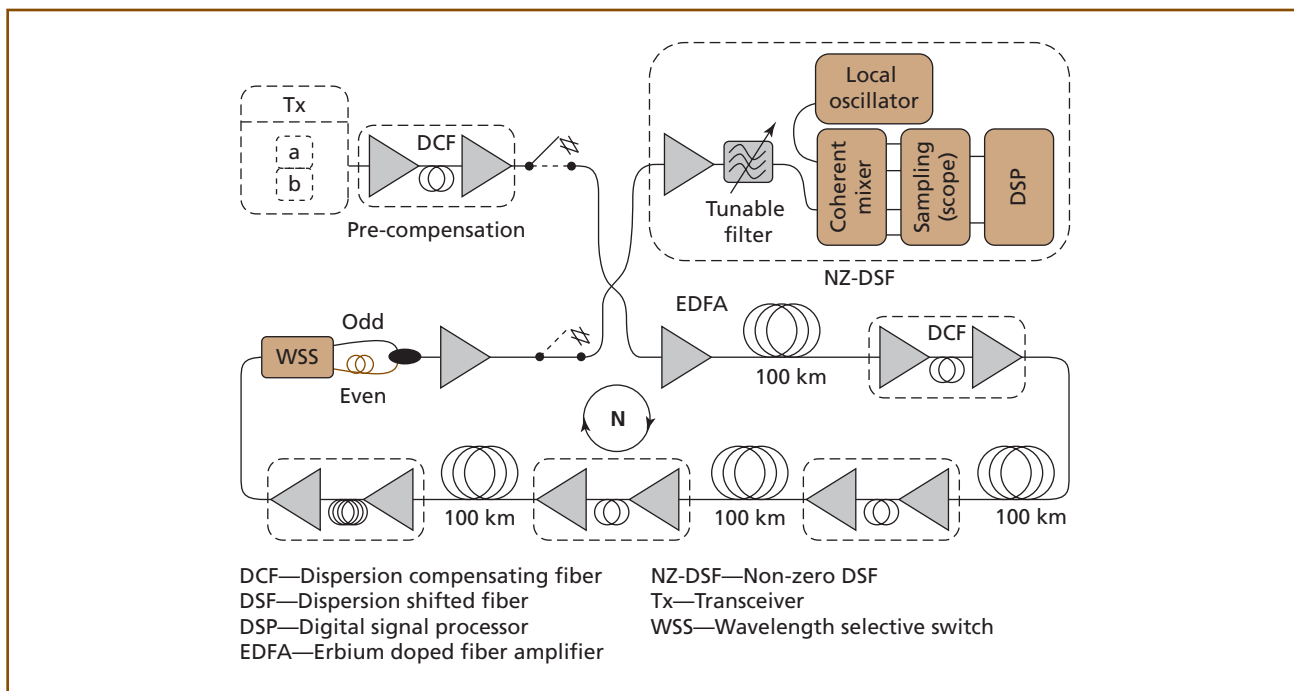


**Figure 9.**  
*Experimental testbed using a recirculating loop.*



experiments, four sets of 2,000,000 samples will be stored for each measurement in order to measure BERs lower than  $10^{-5}$ , corresponding to  $Q^2$  factors of 12.6 dB. Due to polarization scrambling, each recording corresponds to an arbitrary received state of polarization, and BER is computed offline through the four sets of 2,000,000 of samples for each measurement and is subsequently transformed into a  $Q^2$  factor.

### Impact of Intra-Channel Effects in Experimental Results

One of the primary advantages of PDM-QPSK paired with coherent detection is that its sensitivity to optical noise is very close to the lowest value recorded among all modulation schemes. **Figure 10** compares the measured optical noise sensitivity and

the transmission performance obtained for *i*RZ-PDM-QPSK and NRZ-PDM-QPSK. Figure 10a depicts the optical noise sensitivity measured for 100 Gb/s *i*RZ-PDM-QPSK (with triangles) and NRZ-PDM-QPSK (with circles). As can be seen, both solutions provide very similar sensitivity to optical noise. Contrary to directly detected systems in which RZ pulse carving usually improves sensitivity to optical noise, coherent systems perform a digital equalization which compensates for non-perfectly matched filtering, so that the benefit of using RZ pulse carving with respect to NRZ pulse shaping vanishes [18].

We now study and compare the tolerance of 100 Gb/s *i*RZ-PDM-QPSK and NRZ-PDM-QPSK to intra-channel nonlinear effects through a single-channel

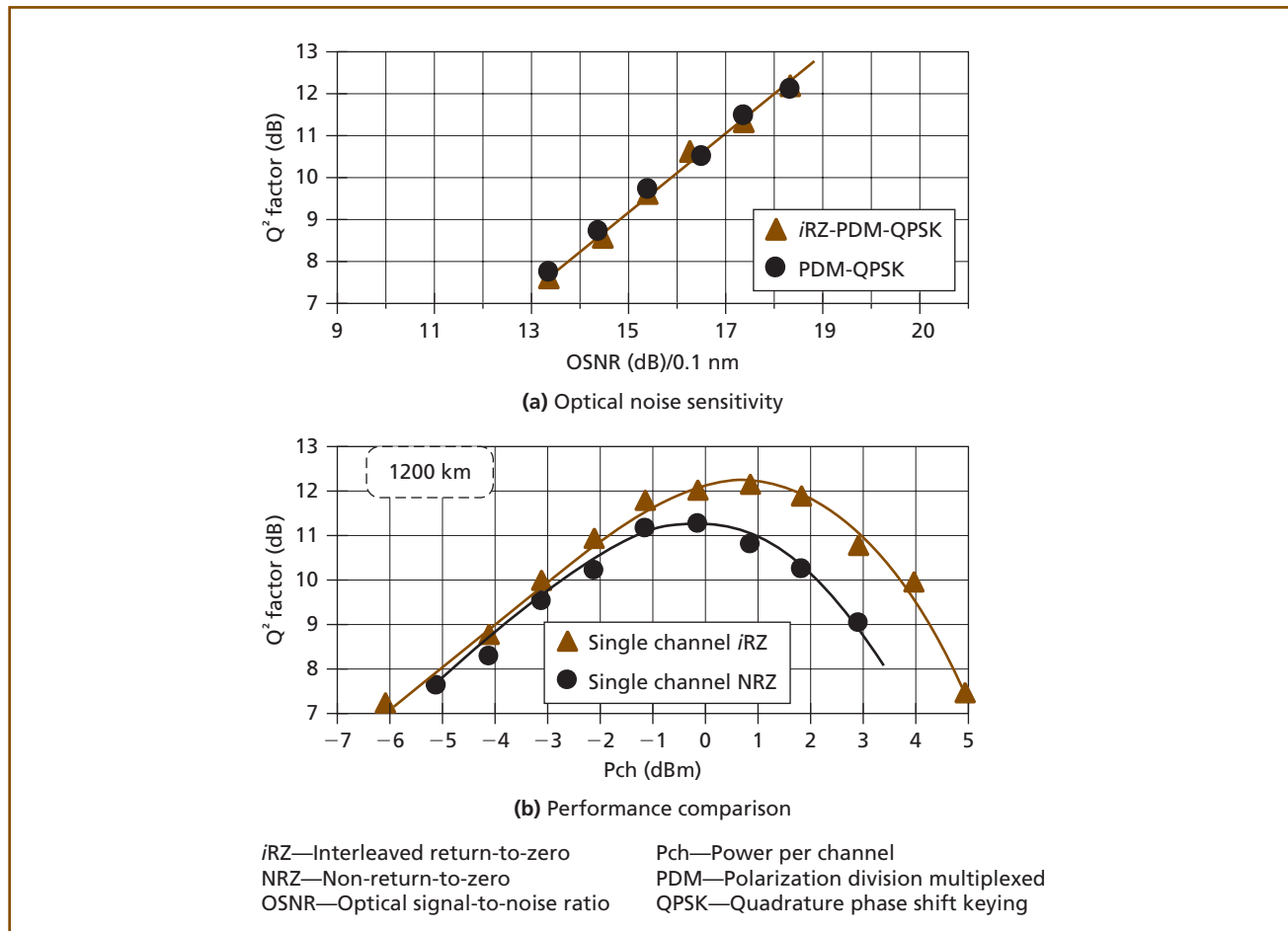


**Figure 10.** Optical noise sensitivity and performance comparison between *i*RZ-PDM-QPSK and NRZ-PDM-QPSK after 1200 km of single-channel transmission.

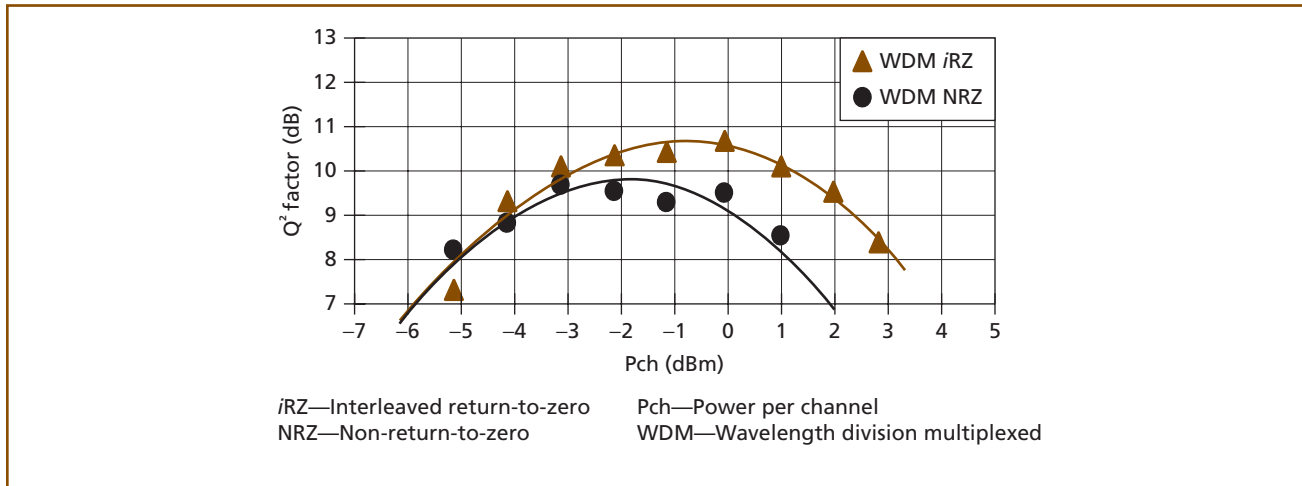


**Figure 11.**  
Tolerance to cross nonlinear effects in a homogeneous WDM transmission after 1200 km.

transmission, i.e., keeping surrounding channels continuous (as illustrated in Figure 7a). Figure 10b shows the performance of the test channel measured after a transmission distance of 1200 km as a function of the power launched per channel, Pch, for *i*RZ-PDM-QPSK (with triangles) and NRZ-PDM-QPSK (with circles). In both cases, for low values of Pch, performance is limited by optical noise and improves as far as optical signal-to-noise ratio (OSNR) is increased when increasing Pch. The intra-channel effects—here, mainly self-phase modulation (SPM) and nonlinear phase noise—arise for both studied solutions as soon as the launch power exceeds  $-1$  dBm. However, the performance of NRZ-PDM-QPSK reaches an optimum for a launch power of 0 dBm whereas the performance of *i*RZ-PDM-QPSK continues to increase up to  $+1$  dBm launch power. This higher tolerance of *i*RZ-PDM-QPSK against intra-channel nonlinear effects brings a 1 dB  $Q^2$  factor benefit as compared to NRZ-PDM-QPSK. This improvement of the tolerance to intra-channel nonlinearities is attributed to the low peak-to-average power ratio obtained by combining polarization interleaving and RZ pulse-carving that reduces nonlinear impairments induced by Kerr effect. It must be pointed out that this benefit has not been observed when both polarizations were RZ-QPSK pulse-to-pulse aligned [19].

### Impact of Inter-Channel Effects in Experimental Results

Here, we measure the performance of one 100 Gb/s *i*RZ-PDM-QPSK channel surrounded by other 100 Gb/s *i*RZ-PDM-QPSK (corresponding to the transmitter configuration depicted in Figure 7b) while varying the channel power launched per span. **Figure 11** shows the performance evolution of the test channel versus the power launched per channel in homogeneous WDM transmission measured after 1200 km. In this figure, it can be seen that the presence of WDM neighboring channels reduces the optimum  $Q^2$  factor by about 1.5 dB compared to the single-channel optimum performance for both *i*RZ-PDM-QPSK and NRZ-PDM-QPSK. This indicates that system penalties brought by WDM nonlinear impairments are similar for both solutions. Thus, the benefit of using *i*RZ-PDM-QPSK as compared to NRZ-PDM-QPSK is mainly related to the mitigation of intra-channel impairments. Besides, the 1.5 dB penalties stemming from inter-channel impairments are not much larger than that observed over SSME, or around 1 dB [19]. This is attributed to the fact that despite the relatively low chromatic dispersion of the NZ-DSF, the walk-off between channels operating at 28 Gbaud is sufficiently high to avoid suffering large penalties induced by cross-channel nonlinear effects. Finally, this experiment demonstrates the feasibility of transmitting

100 Gb/s channels with a spectral efficiency of 2 bit/s/Hz by using coherent detection and the PDM-QPSK format. This transmission experiment paves the way for WDM optical systems of 8 Tb/s capacity over transmission links of more than 1000 km relying on NZ-DSF and including ROADMs.

## Conclusion

The potential of combining coherent detection with advanced modulation formats and digital signal processing to increase information spectral density in optical fiber communication systems has been presented in this paper. Benefiting from powerful digital signal processing, coherent receivers provide unprecedented efficiency to combat optical noise and to mitigate linear fiber impairments such as chromatic dispersion and polarization mode dispersion. Hence, coherent detection used with the 100 Gb/s PDM-QPSK modulation format exhibits a resilience to PMD amounts greater than that required in conventional 10 NRZ systems, or typically around 12 ps. The tolerance to intra-channel and inter-channel nonlinear impairments of the 100 Gb/s coherent PDM-QPSK solution has also been investigated through an 8 Tb/s WDM transmission experiment over a dispersion-managed link based on low dispersion fiber, with either NRZ-PDM-QPSK or *i*RZ-PDM-QPSK modulation. The *i*RZ-PDM-QPSK configuration has been shown to be an attractive solution for long-haul transmission of 100 Gb/s data. Most of all, the transport of  $80 \times 100$  Gb/s channels with spectral efficiency of 2 bit/s/Hz over transmission links of more than 1000 km relying on NZ-DSF and including ROADMs has been demonstrated by using coherent detection and the PDM-QPSK format, paving the way for the capacity upgrade of deployed WDM optical systems.

## References

[1] M. S. Alfiad, D. van den Borne, T. Wuth, M. Kuschnerov, B. Lankl, C. Weiske, E. de Man, A. Napoli, and H. de Waardt, "111-Gb/s POLMUX-RZ-DQPSK Transmission over 1140 km of SSMF with 10.7-Gb/s NRZ-OOK Neighbours," Proc. Eur. Conf. on Optical Commun. (ECOC '08) (Brussels, Belg., 2008), paper Mo.4.E.2.

[2] M. Bertolini, P. Serena, G. Bellotti, and A. Bononi, "On the XPM-Induced Distortion in

DQPSK-OOK and Coherent QPSK-OOK Hybrid Systems," Proc. Optical Fiber Commun. Conf. (OFC '09) (San Diego, CA, 2009), paper OTuD4.

[3] O. Bertran-Pardo, J. Renaudier, G. Charlet, H. Mardoyan, P. Tran, and S. Bigo, "Nonlinearity Limitations When Mixing 40-Gb/s Coherent PDM-QPSK Channels with Preexisting 10-Gb/s NRZ Channels," IEEE Photonics Technol. Lett., 20:15 (2008), 1314–1316.

[4] O. Bertran Pardo, J. Renaudier, G. Charlet, P. Tran, H. Mardoyan, M. Salsi, and S. Bigo, "Impact of Nonlinear Impairments on the Tolerance to PMD of 100 Gb/s PDM-QPSK Data Processed in a Coherent Receiver," Proc. Eur. Conf. on Optical Commun. (ECOC '08) (Brussels, Belg., 2008), paper We.3.E.1.

[5] O. Bertran-Pardo, J. Renaudier, G. Charlet, P. Tran, H. Mardoyan, M. Salsi, and S. Bigo, "Experimental Assessment of Interactions Between Nonlinear Impairments and Polarization-Mode Dispersion in 100-Gb/s Coherent Systems Versus Receiver Complexity," IEEE Photonics Technol. Lett., 21:1 (2009), 51–53.

[6] G. Charlet, J. Renaudier, H. Mardoyan, P. Tran, O. Bertran Pardo, F. Verluise, M. Achouche, A. Boutin, F. Blache, J.-Y. Dupuy, and S. Bigo, "Transmission of 16.4 Tbit/s Capacity over 2,550 km Using PDM QPSK Modulation Format and Coherent Receiver," Proc. Optical Fiber Commun./National Fiber Optic Engineers Conf. (OFC/NFOEC '08) (San Diego, CA, 2008), paper PDP3.

[7] G. Charlet, M. Salsi, P. Tran, M. Bertolini, H. Mardoyan, J. Renaudier, O. Bertran-Pardo, and S. Bigo, " $72 \times 100$  Gb/s Transmission over Transoceanic Distance, Using Large Effective Area Fiber, Hybrid Raman-Erbium Amplification and Coherent Detection," Proc. Optical Fiber Commun. Conf. (OFC '09) (San Diego, CA, 2009), paper PDPB6.

[8] T. Duthel, C. R. S. Fludger, D. van den Borne, C. Schulien, E.-D. Schmidt, T. Wuth, E. De Man, G.-D. Khoe, and H. de Waardt, "Impairment Tolerance of 111 Gbit/s POLMUX-RZ-DQPSK Using a Reduced Complexity Coherent Receiver with T-Spaced Equaliser," Proc. Eur. Conf. on Optical Commun. (ECOC '07) (Berlin, Ger., 2007), paper Mo.1.3.2.

[9] C. R. S. Fludger, T. Duthel, D. van den Borne, C. Schulien, E.-D. Schmidt, T. Wuth, J. Geyer, E. De Man, G.-D. Khoe, and H. de Waardt,

- “Coherent Equalization and POLMUX-RZ-DQPSK for Robust 100-Gb Transmission,” *J. Lightwave Technol.*, 26:1 (2008), 64–72.
- [10] R. A. Griffin, R. I. Johnstone, R. G. Walker, J. Hall, S. D. Wadsworth, K. Berry, A. C. Carter, M. J. Wale, J. Hughes, P. A. Jerram, and N. J. Parsons, “10 Gb/s Optical Differential Quadrature Phase Shift Key (DQPSK) Transmission Using GaAs/AlGaAs Integration,” *Proc. Optical Fiber Commun. Conf. (OFC '02)* (Anaheim, CA, 2002), paper FD6-1.
- [11] Institute of Electrical and Electronics Engineers, “An Overview: The Next Generation of Ethernet,” *IEEE 802.3 Higher Speed Study Group—Tutorial*, IEEE 802 Plenary, Atlanta, GA, Nov. 12, 2007, <[http://www.ieee802.org/3/hssg/public/nov07/HSSG\\_Tutorial\\_1107.zip](http://www.ieee802.org/3/hssg/public/nov07/HSSG_Tutorial_1107.zip)>.
- [12] A. Leven, N. Kaneda, U.-V. Koc, and Y.-K. Chen, “Frequency Estimation in Intradynne Reception,” *IEEE Photonics Technol. Lett.*, 19:6 (2007), 366–368.
- [13] D.-S. Ly-Gagnon, S. Tsukamoto, K. Katoh, and K. Kikuchi, “Coherent Detection of Optical Quadrature Phase-Shift Keying Signals with Carrier Phase Estimation,” *J. Lightwave Technol.*, 24:1 (2006), 12–21.
- [14] L. E. Nelson, T. N. Nielsen, and H. Kogelnik, “Observation of PMD-Induced Coherent Crosstalk in Polarization-Multiplexed Transmission,” *IEEE Photonics Technol. Lett.*, 13:7 (2001), 738–740.
- [15] J. G. Proakis and D. G. Manolakis, *Digital Signal Processing: Principles, Algorithms, and Applications*, 3rd ed., Prentice Hall, Upper Saddle River, NJ, 1995.
- [16] J. Renaudier, O. Bertran-Pardo, H. Mardoyan, P. Tran, M. Salsi, G. Charlet, and S. Bigo, “Impact of Temporal Interleaving of Polarization Tributaries onto 100-Gb/s Coherent Transmission Systems with RZ Pulse Carving,” *IEEE Photonics Technol. Lett.*, 20:24 (2008), 2036–2038.
- [17] J. Renaudier, G. Charlet, O. Bertran Pardo, and S. Bigo, “Long-Haul Transmission Systems Involving Coherent Detection for Linear Impairments Mitigation,” *Proc. IEEE/LEOS Summer Topical Meetings (Acapulco, MX, 2008)*, paper WD1.1, pp. 239–240.
- [18] J. Renaudier, G. Charlet, O. Bertran Pardo, H. Mardoyan, P. Tran, M. Salsi, and S. Bigo, “Experimental Analysis of 100 Gb/s Coherent PDM-QPSK Long-Haul Transmission Under Constraints of Typical Terrestrial Networks,” *Proc. Eur. Conf. on Optical Commun. (ECOC '08)* (Brussels, Belg., 2008), paper Th.2.A.3.
- [19] J. Renaudier, G. Charlet, O. Bertran-Pardo, H. Mardoyan, P. Tran, M. Salsi, and S. Bigo, “Transmission of 100 Gb/s Coherent PDM-QPSK over  $16 \times 100$  km of Standard Fiber with All-Erbium Amplifiers,” *Optics Express*, 17:7 (2009), 5112–5117.
- [20] J. Renaudier, G. Charlet, M. Salsi, O. Bertran Pardo, H. Mardoyan, P. Tran, and S. Bigo, “Linear Fiber Impairments Mitigation of 40-Gbit/s Polarization-Multiplexed QPSK by Digital Processing in a Coherent Receiver,” *J. Lightwave Technol.*, 26:1 (2008), 36–42.
- [21] S. J. Savory, “Digital Filters for Coherent Optical Receivers,” *Optics Express*, 16:2 (2008), 804–817.
- [22] S. J. Savory, G. Gavioli, R. I. Killey, and P. Bayvel, “Electronic Compensation of Chromatic Dispersion Using a Digital Coherent Receiver,” *Optics Express*, 15:5 (2007), 2120–2126.
- [23] S. J. Savory, A. D. Stewart, S. Wood, G. Gavioli, M. G. Taylor, R. I. Killey, and P. Bayvel, “Digital Equalisation of 40 Gbit/s per Wavelength Transmission over 2480 km of Standard Fibre Without Optical Dispersion Compensation,” *Proc. Eur. Conf. on Optical Commun. (ECOC '06)* (Cannes, Fr., 2006), paper Th2.5.5.
- [24] M. G. Taylor, “Coherent Detection Method Using DSP for Demodulation of Signal and Subsequent Equalization of Propagation Impairments,” *IEEE Photonics Technol. Lett.*, 16:2 (2004), 674–676.
- [25] D. van den Borne, C. R. S. Fludger, T. Duthel, T. Wuth, E. D. Schmidt, C. Schullien, E. Gottwald, G. D. Khoe, and H. de Waardt, “Carrier Phase Estimation for Coherent Equalization of 43-Gb/s POLMUX-NRZ-DQPSK Transmission with 10.7-Gb/s NRZ Neighbours,” *Proc. Eur. Conf. on Optical Commun. (ECOC '07)* (Berlin, Ger., 2007), paper We7.2.3.
- [26] D. van den Borne, N. E. Hecker-Denschlag, G.-D. Khoe, and H. de Waardt, “Cross Phase Modulation Induced Depolarization Penalties in  $2 \times 10$  Gbit/s Polarization-Multiplexed Transmission,” *Proc. Eur. Conf. on Optical Commun. (ECOC '04)* (Stockholm, Swed., 2004), paper Mo4.5.5.
- [27] A. J. Viterbi and A. M. Viterbi, “Nonlinear Estimation of PSK-Modulated Carrier Phase with Application to Burst Digital Transmission,” *IEEE Trans. Inform. Theory*, 29:4 (1983), 543–551.



*(Manuscript approved August 2009)*

**JÉRÉMIE RENAUDIER** is a research engineer in the Optical Networks research domain at Alcatel-Lucent Bell Labs in Villarsaux, France. He received an M.S. degree in optical communications and networks from the *École Nationale Supérieure des Télécommunications de Bretagne (ENSTB)*, Brest, France, and a Ph.D. in electrical engineering from the *École Nationale Supérieure des Télécommunications (ENST)*, Paris, France. His Ph.D. thesis, carried out at Alcatel Thales III-V Lab, focused on functional mode-locked DBR lasers for telecommunications applications at 40 Gb/s and beyond. He then joined Alcatel-Lucent Bell Labs to work on optical transmission systems in the WDM Transmission Systems Department. His current research interests involve the study of advanced modulation formats—binary phase shift keying (BPSK), APol RZ-DPSK, DQPSK, polarization division multiplexed (PDM) quadrature phase shift keying (QPSK)—together with coherent detection for WDM long haul and ultra long haul transmissions.



**ORIOLE BERTRAN-PARDO** is Ph.D. candidate in the Optical Networks research domain at Alcatel-Lucent Bell Labs in Villarsaux, France. He received his B.S. degree from *Universitat Politècnica de Catalunya (UPC)*, Barcelona, Spain, and his M.S. degree in devices and techniques of communication from *École Nationale Supérieure des Télécommunication (ENST)*, Paris, France. His previous work, at Alcatel-Thales III-V Lab, focused on quantum dot lasers for telecommunication applications. He is currently working toward a Ph.D. degree at Bell Labs France in collaboration with ENST Paris. His Ph.D. thesis focuses on the application of coherent detection for high bit rate optical communication systems. He has authored or co-authored more than 25 refereed papers and conference contributions.



**GABRIEL CHARLET** is a distinguished member of technical staff in the Optical Networks research domain at Alcatel-Lucent Bell Labs, Villarsaux, France. He received an engineering degree from the *École Supérieure d'Optique*, Orsay, France, and joined Alcatel Research & Innovation the following year. Since that time, his work has been focused on WDM transmission systems and he has realized several multi-Terabit/s transmission records. He also addressed



the topic of advanced modulation formats—phase shaped binary transmission (PSBT), DPSK, APol RZ-DPSK, DQPSK, and coherent detection of polarization division multiplexed (PDM) quadrature phase shift keying (QPSK). He is the author of more than 30 patents and nearly a dozen papers in major conferences such as the Optical Fiber Conference (OFC), European Conference and Exhibition on Optical Communication (ECOC), OAA, Optoelectronic and Communications Conference (OECC). In 2007, he received the Fabry de Gramont award for his work on fiber optics communication.

**MASSIMILIANO SALSI** is a research engineer in the Optical Networks research domain at Alcatel-Lucent Bell Labs in Villarsaux, France. He received both the laurea degree in telecommunications engineering (cum laude) and a Ph.D. degree in information technology from the University of Parma, Italy. His current research focus includes WDM systems for submarine transmission and optical coherent detection with digital signal processing.



**HAÏK MARDOYAN** is an engineering technician in the Optical Networks research domain at Alcatel-Lucent Bell Labs in Villarsaux, France. He received the diploma of high-level technician in optics at the Fresnel Institute, Paris, France. During his tenure at Alcatel-Lucent, he has taken part in large-scale experiments in the field of WDM transmissions, both terrestrial and submarine. He is co-author of 12 post deadline papers in major conferences (OFC, ECOC, OAA, and OECC).



**PATRICE TRAN** is an engineering technician in the Optical Networks research domain at Alcatel-Lucent Bell Labs in Villarsaux, France. He received the degree of high level technician in physics and chemistry from the *Association Nationale Pour la Formation Professionnelle des Adultes (AFPA)*, Paris. He worked for several years on high voltage cables before moving to the Alcatel Research & Innovation division in the Photonics Networks Unit at Marcoussis, France. He is currently working on automation and realization of optical test beds in the WDM Transmission Systems Group and he contributed to the record 25 Tb/s transmission realized in 2007.





*SÉBASTIEN BIGO is head of the WDM Dynamic Networks Department at Alcatel-Lucent Bell Labs in Villarceaux, France. He received a graduate degree from the Institut d'Optique, Orsay, France, and a Ph.D. in physics for work devoted to all-optical processing and soliton transmission. He joined Alcatel Research & Innovation's Photonics Networks Unit in Marcoussis, France, while he was still a student at the University of Besançon. His work has included research on high-capacity WDM terrestrial systems, and large-scale demonstration experiments at 10 Gb/s, 40 Gb/s, and 100 Gb/s channel rates. He has authored and co-authored more than 170 journal and conference papers, and 30 patents. With three other colleagues, he authored the reference book, *Erbium-Doped Fiber Amplifiers: Device and System Developments*, published by John Wiley & Sons in 2002. He received the General Ferrié award in 2003 from the French ICT society, and the IEEE/SEE Brillouin award in 2008. ♦*

